frontiers | Frontiers in Environmental Science

TYPE Original Research
PUBLISHED 23 May 2025
DOI 10.3389/fenvs.2025.1570358

OPEN ACCESS

EDITED BY
Chamindra L. Vithana,
Southern Cross University, Australia

REVIEWED BY
Ferdinand J. Dina Ebouel,
Botswana International University of Science and Technology, Botswana
Hong Zhou,
Tongren University, China

*CORRESPONDENCE
Susanne Claudia Möckel,
susanne@lbhi.is

†Deceased

RECEIVED 03 February 2025
ACCEPTED 14 May 2025
PUBLISHED 23 May 2025

CITATION
Möckel SC, Bonatotzky T, Erlendsson E, Álvarez IRC, Mankasingh U and Gísladóttir G (2025) The drowned soil: effects of an Icelandic hydropower reservoir on the soil carbon resource after 24 years of flooding. *Front. Environ. Sci.* 13:1570358. doi: 10.3389/fenvs.2025.1570358

The drowned soil: effects of an Icelandic hydropower reservoir on the soil carbon resource after 24 years of flooding

Susanne Claudia Möckel[1,2]*, Theresa Bonatotzky[2], Egill Erlendsson[2,3], Ivan Rodrigo Casasola Álvarez[2], Utra Mankasingh[1] and Guðrún Gísladóttir[2,3†]

[1]Faculty of Environmental and Forest Sciences, Agricultural University of Iceland, Reykjavík, Iceland, [2]Institute of Life and Environmental Sciences, University of Iceland, Reykjavík, Iceland, [3]Institute of Earth Sciences, University of Iceland, Reykjavík, Iceland

Increasing energy demand propels the construction of river dams and reservoirs for hydropower, raising concerns about environmental and societal ramifications. Ecological effects like river fragmentation, habitat loss, biodiversity decline, and disruptions of biogeochemical cycles have been addressed for several decades. The impact of water impoundment on submerged soils, particularly carbon stocks, is of growing interest. Studies reveal both increases and decreases of carbon stocks in submerged soils, depending on factors such as substrate resilience, water level fluctuations, soil type and submergence duration. This study examines the effects of 24 years of water impoundment on properties of organic and mineral constituents in Andosols under the Blöndulón hydroelectric reservoir in Iceland´s highlands. Submerged soils show higher carbon stocks than reference soils but are depleted in pedogenic minerals ferrihydrite and allophane. Unlike reference soils, where carbon declines with depth, submerged soils display rather uniform carbon distribution. This is likely due to movement of organic material from upper to lower horizons, and carbon additions from decaying vegetation in the years after the impoundment. Importantly, the apparent carbon enrichment of the submerged soils raises concerns about its long-term stability. The depletion of pedogenic minerals ferrihydrite and allophane may render the carbon sensitive to oxidation in the coming decades, particularly when soils are exposed during water level fluctuations. In short, the carbon enrichment of the drowned soils may not be permanent. Assessments of the consequences of water level fluctuations or potential future dam removal need to take the vulnerability of the exposed soils into account and consider the risk of increased carbon emissions from these soils.

KEYWORDS

hydropower reservoirs, submerged soils, carbon stocks, pedogenic minerals, biogeochemical cycles

1 Introduction

Advances towards reaching Sustainable Development Goal 7 (access to affordable, reliable, sustainable and modern energy for all) have been offset by population growth and economic growth. As of 2021, about 675 million people still lacked access to electricity (United Nations, 2023), particularly in least developed countries. This adds significant

momentum to the construction of river dams and artificial water reservoirs for the production of hydropower (Scheffran et al., 2020; Zarfl et al., 2015). In Iceland, the increasing electricity demand of recent decades has been mainly driven by the heavy industries, which accounted for 78% of electricity consumption in 2021, with the aluminum industry accounting for the greatest share (Orkustofnun, 2022a). In 2021, the share of hydropower in the county´s primary energy use was 20.5% (Orkustofnun, 2023), while hydroelectricity comprised 70% of the electricity produced (Orkustofnun, 2022b).

Although hydropower is often considered a renewable source of sustainable and clean energy, concerns about its environmental and societal ramifications are growing (Voegeli and Finger, 2021; Mulligan et al., 2020). While often regarded as a low- or even no-carbon source of energy (De Souza, 1996), emerging research has highlighted that the flooding of terrestrial ecosystems by hydropower reservoirs disrupts biogeochemical cycles, potentially enhancing greenhouse gas (GHG) emissions in the form of CO_2 and CH_4 from hydroelectric reservoirs (e.g., Félix-Faure et al., 2019b; Félix-Faure et al., 2019a; Oelbermann and Schiff, 2010; Oelbermann and Schiff, 2008; Wang et al., 2024). Emissions are largely driven by the increased vulnerability of soil organic C to mineralization upon artificial water impoundment and by the decomposition of inundated vegetation (Oelbermann and Schiff, 2010; Huttunen et al., 2002; Oelbermann and Schiff, 2008). Variability in emission rates is great, though. A recent review of GHG emissions from hydropower schemes (Wang et al., 2024) revealed higher emissions per unit area from small than large hydropower reservoirs in most climatic zones, not least in boreal areas. A range of other factors, such as temperature, the response of different microbial communities to disturbance (Unger et al., 2009), availability of nutrients and alternative electron acceptors (Zhang et al., 2021), water residence time, reservoir depth, magnitude of water level drawdowns, fluctuations in redox potential (Wang et al., 2024), and soil type also play a role.

Loss of C from submerged soils can be substantial, but the fate of soils and the stability of their C stocks upon reservoir flooding, appears to be driven by a combination of soil internal and external factors. A study in France revealed a soil loss of about 40 cm, or, in other words, the loss of the O and A horizons of Podzols in the annual drawdown zone of a reservoir after about 80 years of flooding (Félix-Faure et al., 2019b). Permanently flooded parts of the area also lost a substantial part of the O horizon. Such loss of organic surface horizons naturally translates into significant losses of C. Studying Cambisols after about 80 years of water impoundment, Félix-Faure et al. (2019a) showed a loss of about 50% of the original soil C, indicating significant mineralization rates even under permanent submersion. Oxygen saturation of the water may play a role here. Some parts of reservoirs, particularly those close to the main inlet and where the water depth is shallow, can be oxic for a major part of the year. A decrease in C concentration is not observed in all studies on artificially submerged soils. Oelbermann and Schiff (2010) found increases in C concentrations after 5 years of episodic flooding in the Experimental Lakes Area in Ontario, Canada, along with a redistribution of C from surface layers, decaying plant biomass, and more organic soil horizons, into deeper soil layers. The substantial difference in submergence time between the studies of Félix-Faure et al. (2019b) (approximately 80 years) and Oelbermann and Schiff (2010) (5 years) likely explains the contradictory results of soil C loss versus C gain. Importantly, C of recently flooded soil might be particularly sensitive to oxidation due to high sources of labile soil organic matter (SOM) and nutrient release from the inundated terrestrial vegetation (Huttunen et al., 2002; Oelbermann and Schiff, 2008). Moreover, hydropower reservoirs not only influence the drowned soils, but also soils in the shoreline and near environment of the reservoir. Shore erosion is a known problem around artificial reservoirs. Vilmundardóttir et al. (2010) described significant erosion and redeposition of Andosols at the shoreline of the Blöndulón reservoir in North Iceland, governed by a combination of substrate resilience, wind strength and direction, fetch length and resulting wave power, and water level. Eroding soil material along the shoreline, and soil material and sediments from the annual drawdown zone can then be driven by wind and form advancing sand fronts (Vilmundardóttir et al., 2010). These move over vegetated areas, thereby suffocating and uprooting vegetation, leaving barren areas (Arnalds, 2015).

To elucidate the implications of submergence on C in drowned soils, an understanding of the mechanisms of C stabilization in the affected soils is required. Accumulation and stabilization mechanisms of soil organic C differ substantially between soil groups, e.g., due to external factors such as climate, but also due to distinct physicochemical soil properties derived from pedogenesis; steering, amongst others, aggregate formation and the availability of reactive mineral surfaces, and active metal ions (Kögel-Knabner and Amelung, 2021). Andosols, soils which predominantly form from volcanic ejecta such as those in Iceland, are known for their exceptionally high C storage capabilities (Wada, 1985; Takahashi and Dahlgren, 2016), due to the following stabilization mechanisms: The weathering of the volcanic parent material leads to abundant precipitation of aluminium (Al), iron (Fe) and silicon (Si), which favors the formation of highly active nanocrystalline minerals like the aluminosilicate allophane and the Fe-hydroxide ferrihydrite (Bonatotzky et al., 2021; Hewitt et al., 2021; Shoji et al., 1993; Wada, 1989; Kögel-Knabner and Amelung, 2021). Through the formation of organo-mineral complexes facilitated by their reactive surfaces, these clay-sized mineral constituents play a strong role in C accumulation in Andosols (Kögel-Knabner et al., 2008; Kleber et al., 2005; Rasmussen et al., 2018). Also, complexation of metal ions, particularly Al but also Fe, with humus plays an important role, particularly in non-allophanic Andosols (Inagaki et al., 2020), as well as physical protection within micropores (Asano and Wagai, 2014).

Long-term flooding as a strong form of environmental disturbance could lead to the destabilization of pedogenic minerals, metal-humus complexes, and soil aggregates, and eventually render the C of the drowned soils more sensitive to loss. Under reducing conditions, iron oxides like ferrihydrite become unstable due to the reduction of Fe(III) to more soluble Fe(II). The resulting decrease in Fe(III)-bearing iron oxide content (Félix-Faure et al., 2019b) can cause the loss of C once stabilized in Fe(III)-organic complexes (Knorr, 2013; Chen et al., 2020; Inagaki et al., 2020). Reduction of Fe and the loss of Fe minerals from submerged soils is, e.g., demonstrated by Banach et al. (2009), who describe increased mobilization of Fe(II) after only few weeks of inundation in a mesocosm experiment. A study on soil water quality

of the Nam Theun 2 Reservoir in Laos by Chanudet et al. (2016) showed an over threefold increase in dissolved iron concentrations downstream during the first 5 years of impoundment. Contrary to Fe, Al is not redox active in soils (Strawn et al., 2015). Hence, aluminosilicates such as allophane, and Al-humus complexes might retain their C stabilizing role under reducing conditions (Inagaki et al., 2020). However, allophane also contributes to C stabilization through the formation of silt sized aggregates and microcompartments in which SOM can become trapped (Filimonova et al., 2016). Aggregate stability of Andosols is generally known to be high (Candan and Broquen, 2009; Buytaert et al., 2006), but strong environmental disturbance, like decades of flooding and frequent water level fluctuations, as in the annual drawdown zone of reservoirs, could lead to the destruction of soil aggregates (Zhu et al., 2022).

The aim of this research was to shed light on the influence of artificial flooding by hydropower reservoirs on properties of organic and mineral soil constituents in Andosols and to evaluate the potential consequences for the C balance of the submerged soils. The following research objectives were at the core of the study:

1. To compare properties of organic and mineral soil constituents of submerged soils with those of non-flooded reference soils in the vicinity of the reservoir.
2. To compare C stocks of submerged soils with those of non-flooded reference soils in the vicinity of the reservoir.
3. To reveal implications of potential changes in soil properties after several decades of flooding for the C balance of the submerged soils, particularly when they are subject to water level changes.

2 Research setting

The study area is located at the margin of the highlands in northern Iceland, around the Blöndulón hydroelectric storage reservoir (Figure 1). The hydroelectric power station Blöndustöð started operations in 1991, with the damming of the glacial river Blanda and flooding of the surrounding areas. The overfall of Blöndulón reservoir is at 478 m above sea level (a.s.l.), and the reservoir covers an area of approximately 57 km^2 when the water table is at overfall height. The water level undergoes annual fluctuations; the level is lowest in spring, primarily March and April, while maximum water level heights are common in late summer and early fall (August–October, Figure 2). The climate in the area is rather dry. Mean annual precipitation is around 400 mm, with highest precipitation in July, August, and September (Figure 3C). Mean annual temperature is around 0.7°C, with highest mean temperature in July (8.7°C, Figure 3B) and lowest mean temperature in February (−5°C). The predominant wind direction in the area is SSE, and the mean wind speed is 7.6 m s^{-1} (Figure 3A). While there were barren stretches along ridges and riverbeds, the area was comparatively well vegetated prior to the artificial flooding. The vegetation was dominated by *Racomitrium* heath communities, dwarf shrub heaths, grasslands, bogs, and fens (Agricultural Research Institute, 1970). Soil erosion had been an ongoing challenge in the area since long before the formation of the reservoir (Arnalds et al., 2001; Kaldal and Víkingsson, 1982). Following the Icelandic Soil Classification and the Icelandic soil map (Arnalds and Óskarsson, 2009), the soils in the area are dominated by Histic and Gleyic Andosols in wetlands, and Brown Andosols in vegetated drylands, whereas Cambic Vitrisols and Arenic Vitrisols occur in unvegetated patches. The soil depth in the reservoir was around 0.5–1 m in vegetated drylands, whereas 2–3 m were common in wetlands prior to the flooding (Kaldal and Víkingsson, 1982; Kristinsson and Hallgrímsson, 1978).

3 Methods

3.1 Soil sampling and site descriptions

The sampling sites were selected to cover the main soil types in the area. Six locations under the reservoir representing the dominant ecosystem types (and hence soil types) were chosen based on vegetation maps made prior to the reservoir by the ARI (Agricultural Research Institute, 1970). Sampling of flooded soils was conducted in winter 2015. From each of the six sites, nine replicate cores over 30 cm deep were retrieved by coring. The coring took place on ice during winter, using a Bolivia-adapted Livingstone piston corer, and polycarbonate tubes with 7 cm inner diameter and length to retrieve 150 cm long soil/sediment cores (e.g., Wright, 1967). About 25 cm wide holes were made through the ice at each sampling location using an ice drill, water depth measured and the polycarbonate tubes pushed into the soil. When the tubes were pulled out, the piston created vacuum within the tubes to prevent movement and mixing of material within them. Upon retrieval, each tube was labelled and sealed, then stored at 4°C until laboratory processing began. In the laboratory, the cores were split lengthwise into two equal halves. One-half was sealed and archived, the other used for analyses. Sediments deposited on the surface of the flooded soils were separated from the upper horizon of the submerged soils, based on color, texture and structure. Then, the upper 30 cm of the soil within each core were divided into intervals of 0–5 cm, 5–10 cm, 10–20 cm and 20–30 cm, air-dried and sieved (<2 mm), and the three replicate samples of each depth interval were pooled.

Of the six flooded sites, samples from five sites were used in this study (sites FL1, 2, 3, 4 and 6). Samples from site FL5 were discarded as they only contained water-sediment slurry without recognizable soil. Three of the flooded sites were poorly drained areas prior to the reservoir (FL1, FL2, FL6; Table 1). Site FL1 was likely a *Carex nigra* bog (U5), FL2 either a *Carex rostrata* fen (V2) or an *Eriophorum angustifolium* fen (V3) or a mix of both, and site FL6 likely constituted a *Salix phylicifolia–Carex bigelowii*–bog (U11). The two remaining sites were freely drained ecosystems. Site FL3 probably constituted *Empetrum nigrum–Salix* dominated freely drained land (B3), while site FL4 likely represented *Kobresia myosuroides*–dwarf shrubs freely drained land (E2).

Based on the ARI vegetation maps, six reference sites in the vicinity of the reservoir, with vegetation communities similar to the flooded sites, were selected. Reference soils were sampled from three poorly drained sites marked U11, U5, and V2/V3 on the ARI maps (sites NFL1, NFL2, NFL3, respectively), and from a freely drained E2 dryland (site NFL4). The sites indicated as B3 freely drained drylands in the vicinity of the reservoir were unsuitable as reference

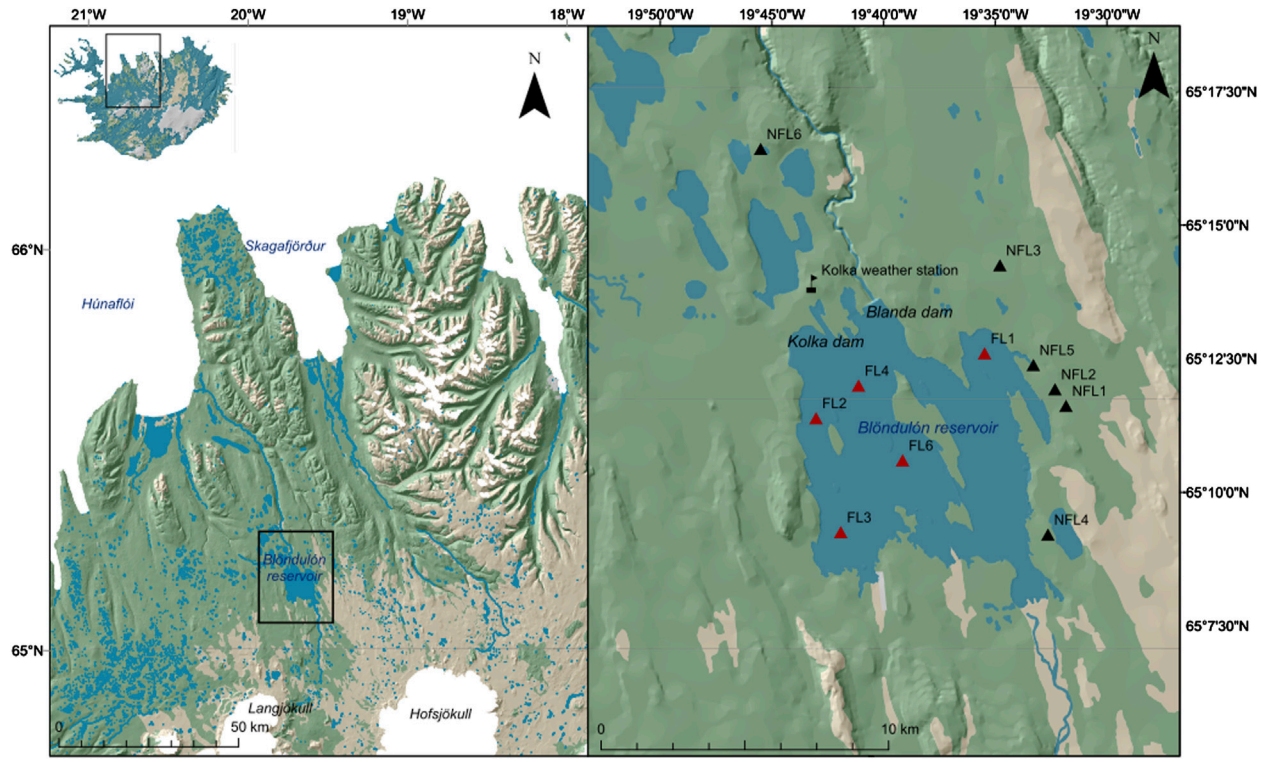

FIGURE 1
The maps show the research area. Sample sites within the reservoir (FL) are shown by red triangles, reference sites around the reservoir (NFL) are shown by black triangles.

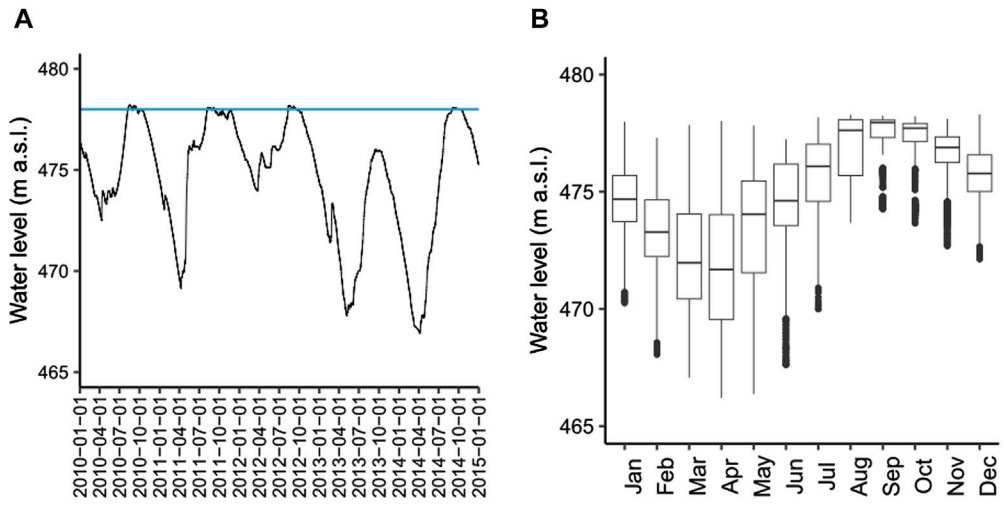

FIGURE 2
(A) Water level fluctuations in Blöndulón hydroelectric reservoir between January 2010 and January 2015, the overfall height at 478 m is indicated as a blue horizontal line. **(B)** Monthly distribution of water level in Blöndulón hydroelectric reservoir in the years 1991–2024. Data from Landsvirkjun (2024).

sites, as many of them were actually mires. Therefore, we decided to collect a reference sample from a grassland (H1; site NFL5). Additionally, we collected young gravelly soils from a riverwash (NFL6). This was decided due to conspicuously low C contents at site FL3, which may indicate that site FL3 was either wrongly marked as B3 on the old vegetation map or very degraded (Arnalds et al., 2001; Kaldal and Víkingsson, 1982).

At each reference site, systematic vegetation description was conducted at nine quadrats (0.25 m^2) along three parallel transects from the margin to the center (resulting in three quadrats each at

10.3389/fenvs.2025.1570358

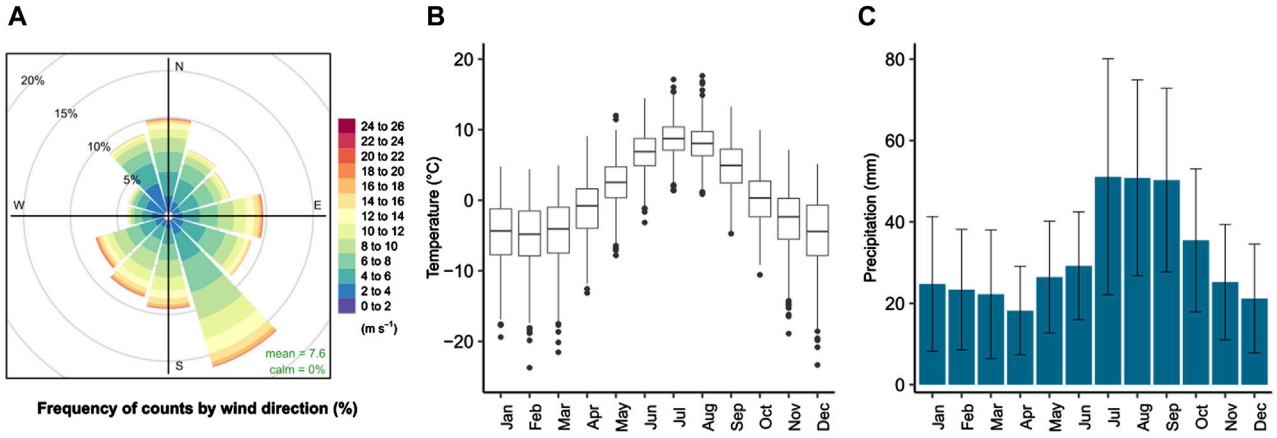

FIGURE 3
The windrose in **(A)** shows main wind direction and wind speeds in the area, **(B)** shows monthly temperature ranges between 1994 and 2023, **(C)** shows monthly precipitation.

TABLE 1 Vegetation communities at our sites prior to reservoir flooding (Agricultural Research Institute, 1970) and according to EUNIS (European Environment Agency, 2019), soil classes according to the Icelandic Soil Classification and Icelandic Soil Map (Arnalds and Óskarsson, 2009; Arnalds, 2015), and soil texture and consistency as key morphological properties. Soil texture and consistency varies with depth, when there is more than one textural class or type of consistency.

Site	Vegetation community prior to reservoir	Vegetation community following EUNIS	Soil class	Texture	Consistency
Sites within reservoir					
FL1	U5 *Carex nigra* bogs	NA	Histic Andosol	lome	friable, firm
FL2	V2/V3 *Carex rostrata* fens/*Eriophorum angustifolium* fens	NA	Gleyic Andosol	loam	very friable, friable
FL3	B3 *Empetrum nigrum* - *Salix* -freely drained land	NA	Vitrisol/Brown Andosol	loam	very friable
FL4	E2 *Kobresia myosuroides* - darf shrubs - freely drained land	NA	Brown Andosol	loam, clay	friable
FL6	U11 *Salix phylicifolia* - *Carex bigelowii* - bogs	NA	Brown Andosol/Gleyic Andosol	loam, sandy loam	friable, firm
Non-flooded reference sites					
NFL1	U11 *Salix phylicifolia* - *Carex bigelowii* - bogs	D2.26 Common cottongrass fens	Gleyic Andosol	loam, clay, silty clay	friable, firm
NFL2	U5 *Carex nigra* bogs	D4.162 Boreal black sedgebrown moss fens	Gleyic Andosol	clay, silt, sand	firm
NFL3	V2/V3 *Carex rostrata* fens/*Eriophorum angustifolium* fens	D2.26 Common cottongrass fens	Histic Andosol/Gleyic Andosol	sandy clay, silty clay, clay	friable, firm
NFL4	E2 *Kobresia myosuroides* - darf shrubs - freely drained land	F2.294 Arctic *Dryas* heaths	Brown Andosol	loamy sand, clay, loam	friable, firm
NFL5	H1 Grassland	E4.28 Icelandic *Racomitrium* grass heaths	Brown Andosol	clay, silty clay	firm
NFL6	Riverwash, wet	L1 Fell fields, moraines and sands	Vitrisol	sand, loamy sand	loose

the margin, at the center, and between the margin and the center of each site) following the Relevé Method by Braun-Blanquet (Mueller-Dombois and Ellenberg, 1974). Plant species were identified using Kristinsson (2010). Soil samples were taken from the rooting zone (top 30 cm; see Iversen et al., 2015) at the three plots of one transect at each site, subdivided into four intervals: 0–5 cm, 5–10 cm, 10–20 cm and 20–30 cm. For the determination of dry bulk density (DBD) and field water content, samples of a predefined volume were taken from each layer. One soil core was retrieved from each site for soil morphological descriptions. All soil samples were subsequently stored at 4°C until further processing. Sampling of reference soils and vegetation analysis took place in June and August 2018, respectively.

According to our own vegetation descriptions at the reference sites, and following the European Nature Information System EUNIS (European Environment Agency, 2019), NFL1 and NFL2 are similar to D2.26 Common cotton-grass fens, NFL2 is similar to D4.162 Boreal black sedge-brown moss fens, Site NFL4 is somewhat similar to F2.294 Arctic *Dryas* heaths, and NFL5 to E4.28 Icelandic *Racomitrium* grass heaths.

3.2 Soil morphology, physical soil properties and pH

Soil texture and consistency were described in the laboratory following Schoeneberger et al. (2012). The DBD was determined by drying soil samples of known volume at 105°C for 24 h and calculating the mass-to-volume ratio of the fine earth fraction (<2 mm). Field water content was calculated based on the mass loss during drying at 105°C for 24 h. Content of SOM and inorganic material (IOM) was determined by loss on ignition at 550°C (Heiri et al., 2001). Soil acidity was measured in deionized water using a soil to water ratio of 1:5 (Blakemore et al., 1987; Rayment and Lyons, 2011).

3.3 Total C and N, $\delta^{13}C$ and $\delta^{15}N$

Values of $\delta^{13}C$ and $\delta^{15}N$ and total C (%C) and nitrogen (%N) were determined on a Thermo Delta V isotope ratio mass spectrometer (IRMS) interfaced to a NC2500 elemental analyzer at the Cornell Isotope Laboratory in the USA. $\delta^{13}C$ values are expressed relative to the Vienna Pee-Dee Belemnite standard and reported in delta notation (‰), while $\delta^{15}N$ values are expressed relative to the atmospheric N standard and reported in delta notation (‰). Due to the absence of carbonate minerals in Icelandic soils (Vilmundardóttir et al., 2014), we assumed soil organic C to be equivalent to %C. This assumption was confirmed by determining soil inorganic C in a selected subset of samples. As a proxy for decomposition (e.g., Malmer and Holm, 1984; Kuhry and Vitt, 1996) we calculated the molar C/N ratio. Based on DBD and %C, we calculated the C density (kg m^{-3}) and C stocks (kg m^{-2}) for each depth interval.

3.4 Permanganate oxidizable carbon

Two fractions of permanganate oxidizable C were determined using two concentrations of $KMnO_4$ solution and different reaction times. Both methods are based on the assumption that 1 mM of $KMnO_4$ oxidizes 9 mg of C (Tirol-Padre and Ladha, 2004; Weil et al., 2003).

To estimate the biologically active soil organic C pool, soil organic C oxidized by a 0.02 M $KMnO_4$ solution was determined following Weil et al. (2003). Briefly, between 0.5 and 2.5 g of soil (depending on C content) was mixed with 20 mL of 0.02 M $KMnO_4$ in 50 mL centrifuge tubes. The tubes were shaken for exactly 2 min (200 rpm) and centrifuged for 9 min at 5,000 rpm. Then, 0.5 mL of the supernatant were diluted to 50 mL with deionized water, and sample absorbance was read at 550 nm using a Genesys10S UV-vis spectrophotometer, Thermo Scientific, USA. Absorbance values were compared with a standard curve derived from known $KMnO_4$ concentrations. The C fraction extracted by 0.02 M $KMnO_4$ is hereafter called POX_{02}-C.

The fraction of organic C suggested to represent a slower pool of C (Tirol-Padre and Ladha, 2004), was determined by oxidizing organic C for 24 h using 33 mM $KMnO_4$. Samples of soil containing 15 mg C were mixed with 25 mL of 33 mM $KMnO_4$ solution in centrifuge tubes and shaken for 24 h, at 12 rpm. After centrifugation for 5 min at 2000 rpm, 2 mL of the supernatant were diluted to 50 mL with deionized water and the absorbance at 565 nm recorded (Genesys10S UV-vis spectrophotometer, Thermo Scientific, USA). Blank samples, containing no soil were analyzed in each run. The concentration of $KMnO_4$ solution mixed with soils and of the blanks was calculated from a standard calibration curve, for which the range for the standards was chosen to adequately cover the sample range. The C fraction extracted by 33 mM $KMnO_4$ is hereafter called POX_{33}-C.

3.5 Microbial biomass carbon

Microbial biomass C (MBC) was determined by chloroform fumigation based on Vance et al. (1987). Four replicates of each soil sample (<2 mm, air-dried) were rewetted to field-moisture content and incubated for 12 days at 25°C. Additionally, four replicates of a combusted soil sample (with no C) were incubated as a matrix blank. The use of a matrix blank is important to subtract any potential chloroform-derived C, which may be adsorbed to pedogenic minerals after fumigation (Alessi et al., 2011). After day 12, two replicate soil samples and two matrix blank samples were chloroform fumigated under vacuum at 25°C for 48 h. After fumigation, samples were mixed with 0.5 M K_2SO_4 (1:4 ratio of soil to K_2SO_4), shaken for 30 min at 120 rpm, and filtered (Whatman No. 42). The two non-fumigated replicate soil samples were also extracted with K_2SO_4. The extracts from all samples were analyzed for total organic carbon (TOC) and total nitrogen (TN). Microbial biomass C was calculated as blank corrected difference in TOC between the fumigated and the non-fumigated samples, divided by a conversion factor k = 0.45 (Vance et al., 1987). The TOC of the non-fumigated soils extracted with 0.5M K_2SO_4 was considered to be a measure of the labile C pool of the soils (Guicharnaud et al., 2010). This C fraction is hereafter called K_2SO_4-C.

3.6 Amorphous Al and Fe phases, and Al and Fe in organic complexes

Selective dissolution of Al, Fe and Si with ammonium oxalate (0.2 M, pH 3.0), was carried out following Soil Survey Staff (2014; method 4G2). The Al, Fe and Si thus extracted (Al_o, Fe_o, Si_o) are indicative of the active forms of Al and Fe of organic complexes (Al/Fe-humus complexes), nanocrystalline hydrous oxides of Fe and Al, and aluminosilicates like allophane (Nanzyo et al., 1993; Wada, 1989). Sodium pyrophosphate was used to extract the part of active Fe and Al (Fe_p, Al_p), which is associated with organic compounds (Al/Fe-humus complexes; Soil Survey Staff, 2014; method 4G3). The sum of Al_o + ½Fe_o was calculated as a diagnostic criterion of andic

soil properties (≥2%; IUSS Working Group Wrb, 2022). Ferrihydrite was estimated as %ferrihydrite = $\%Fe_o$ x 1.7 (Childs, 1985). Allophane or allophane-like constituents were estimated by the equation proposed by Mizota and van Reeuwijk (1989), based on Parfitt and Wilson (1985).

3.7 Statistics

The distribution and means of %C, C densities, C stocks, C/N ratios, pH, DBD, POX_{33}-C, POX_{02}-C, MBC, K_2SO_4-C, and allophane and ferrihydrite as a ratio of C (allophane/carbon, ferrihydrite/carbon) in flooded soils and references soils were illustrated by boxplots. To determine if there were statistically significant differences between group means, an unpaired t-test was performed for normally distributed variables, while a Wilcoxon rank sum test was performed for non-normally distributed variables.

The variation in organo-mineral composition between the soils as reflected by POX_{33}-C, POX_{02}-C, MBC, K_2SO_4-C, allophane and ferrihydrite was visualized by ordination. The six variables were normalized to C content and treated as one multivariate compositional data set (van den Boogaart and Tolosana-Delgado, 2013). After detection of several multivariate outliers (R package robCompositions function out CoDa; Filzmoser et al., 2018; Templ et al., 2011) and replacement of rounded zeros (Martín-Fernández et al., 2012) using the function impRZilr (method "MM"), robust principal component analysis for compositional data was performed (R package robCompositions, function pcaCoDa). The PCA was conducted on isometric logratio coordinates (ilr), and the loadings and scores were back-transformed into centered logratio (clr) space to facilitate graphical illustration and interpretation of the results. Several external variables, which shed better light on the physicochemical properties of the soils were also included in the PCA, namely, Box-Cox transformed C/N ratios, log-transformed DBD, and pH. The external variables were centered and scaled prior to analysis.

After PCA, we investigated possible predictors of variations in POX_{33}-C, which had a) high loadings in the first two dimensions of the PCA and b) represented the greatest share of total carbon content. We performed multivariate beta regression (R package betareg, function betareg; Cribari-Neto and Zeileis, 2010) with POX_{33}-C, expressed as a proportion of total C content, as a continuous response variable bounded by 0 and 1. Variables which showed high loadings in the PCA were selected as predictors, namely, allophane and ferrihydrite (as a ratio of total carbon content), pH and C/N ratios. Predictors with a highly right-skewed distribution (allophane and ferrihydrite) were log-transformed. Several models with different combinations of linear predictors were applied. Aikaike Information Criterion (AIC) was used to select the best-fit model.

4 Results

4.1 Soil characteristics

Soil characteristics for the non-flooded reference sites and the flooded sites are provided in Table 2 and Table 3 respectively. The dominant soil textural class at the flooded sites was loam, whereas the consistency of most flooded soil samples was friable to very friable. Some samples showed firm consistency (0–5 cm at FL1 and 10–20 cm and 20–30 cm at FL6). The soil texture of the reference soils was dominated by sand at NFL6 and silty clay at NFL5. At NFL1-4, the texture was more variable across depth increments. NFL1 comprised generally fine textured soils (loam, clay and silty clay). NFL2 showed more variable texture ranging from clay to silt and sand. NFL3 was dominated by clay textural classes, including sandy and silty clay. NFL4 was comprised of loamy sand, clay and loam. The dominant consistency of the reference soils was friable and firm at sites NFL1, NFL3 and NFL4, firm at sites NFL2 and 5 and loose at NFL6.

Carbon content at the flooded sites was highest at FL1 ($\bar{x}$ = 12.6%), FL2 ($\bar{x}$ = 10.8%) and FL6 ($\bar{x}$ = 10.8%), which comprised poorly drained land before flooding. At the same time, these sites revealed low DBD ($\bar{x}$ = 0.4 g cm^{-3}, 0.5 g cm^{-3} and 0.6 g cm^{-3}, respectively) and low pH values ($\bar{x}$ = 5.5, 5.5 and 5.6, respectively). The freely drained sites, FL3 and FL4, showed more variable soil characteristics, with C contents of $\bar{x}$ = 1.6% and 7.4%, respectively, DBD of $\bar{x}$ = 1.1 g cm^{-3} and 0.7 g cm^{-3}, respectively and pH of $\bar{x}$ = 6.1 and 6.2, respectively. Following the Icelandic Soil Classification, soil classes at the flooded sites included Histic Andosols (12%–20% C; FL1) and Gleyic Andosols (<12% C, FL2 and FL6) in poorly drained land, and Brown Andosols (<12% C; FL4) and Vitrisols (<1.5% C; FL3) in freely drained land (Tables 1, 3; Arnalds, 2015; Arnalds and Óskarsson, 2009).

At the reference sites, the C content was highest at the poorly drained site, NFL 3 ($\bar{x}$ = 11.1%) while DBD was lowest ($\bar{x}$ = 0.4 g cm^{-3}). The other two poorly drained sites, NFL1 and NFL2, showed considerably lower C contents ($\bar{x}$ = 4.1% and 4.4%) and higher DBD ($\bar{x}$ = 0.7 g cm^{-3} at both sites). The pH values at the poorly drained sites were $\bar{x}$ = 5.6 at NFL2 and NFL3, and 6 at NFL1. The riverwash site, NFL6, showed the lowest C contents of all sites ($\bar{x}$ = 0.6%), and comparatively high DBD ($\bar{x}$ = 1.1) and pH ($\bar{x}$ = 6.4). The freely drained vegetated sites, NFL4 and NFL5, showed intermediate C contents ($\bar{x}$ = 4.3% and 3.0%), DBD ($\bar{x}$ = 0.7 g cm^{-3} and 0.8 g cm^{-3}) and pH ($\bar{x}$ = 6.4 and 6.3). Following the Icelandic Soil Classification, soils at the poorly drained reference sites NFL1-3 were classified as Histic and Gleyic Andosols, Brown Andosols at freely drained sites NFL4 and NFL5, and Vitrisols at the riverwash site, NFL6 (Tables 1, 2; Arnalds, 2015; Arnalds and Óskarsson, 2009).

4.2 Carbon and mineral soil characteristics of flooded compared to reference soils

There are clear differences in soil properties between flooded and reference soils (Figure 4; Tables 2, 3). Relative C content (%C), C densities, C stocks, C/N ratios and POX_{33}-C were significantly higher in the flooded soils than the reference soils. For example, average C content in the flooded soils was 8.66% compared to 4.59% in the reference soils. C density averaged 47.0 kg m^{-3} in the flooded soils, while it was 26.4 kg m^{-3} in the reference soils. POX_{33}-C averaged 436 g kg_{carbon}^{-1} in the drowned soils, but 201 g kg_{carbon}^{-1} in the reference soils.

Ferrihydrite and allophane as a ratio of C (ferrihydrite/carbon, allophane/carbon), MBC and pH were significantly lower in the soils from the reservoir than the reference soils (Figure 4). For instance,

TABLE 2 Soil properties of non-flooded reference soils. Site means and standard deviations (SD) for each variable and site are included in bold (weighted according to thickness of depth interval of each observation).

Site	Depth cm	POX_{02}-C	POX_{33}-C	MBC	K_2SO_4-C	C (%)	N (%)	C/N	DBD	SOM	pH	Allophane	Ferrihydrite	C Density	C Stock	$\delta^{13}C$	$\delta^{15}N$
		g kg_{carbon}^{-1}				%	%	molar ratio	g cm^{-3}	%		%	%	kg m^{-3}	kg m^{-2}	‰	‰
NFL 1	0–5	33.3	295	5.78	8.36	6.44	0.47	16	0.50	16.38	5.89	7.44	4.71	32.30	1.62	−26.70	1.55
NFL 1	5–10	24.9	210	3.84	6.62	3.83	0.29	15	0.66	10.63	5.97	8.06	4.79	25.33	1.27	−25.99	1.54
NFL 1	10–20	26.1	179	1.67	5.30	3.11	0.24	15	0.79	8.22	6.07	9.16	5.52	24.46	2.45	−25.76	1.16
NFL 1	20–30	21.6	185	4.51	5.52	4.10	0.32	15	0.68	10.10	6.06	5.86	4.84	27.72	2.77	−26.03	1.57
Weighted site mean		**25.6**	**205.7**	**3.7**	**6.1**	**4.1**	**0.3**	**15.2**	**0.7**	**10.6**	**6.0**	**7.6**	**5.0**	**27.0**	**2.2**	**−26.0**	**1.4**
Weighted SD		**4.5**	**47.5**	**1.8**	**1.3**	**1.3**	**0.1**	**0.4**	**0.1**	**3.2**	**0.1**	**1.6**	**0.4**	**3.2**	**0.7**	**0.4**	**0.2**
NFL 2	0–5	33.5	300	4.33	6.34	8.50	0.53	19	0.33	24.52	6.06	3.79	3.88	28.08	1.40	−26.70	0.67
NFL 2	5–10	39.3	258	2.73	4.34	5.71	0.36	18	0.56	13.64	5.61	7.22	6.25	32.18	1.61	−26.96	0.48
NFL 2	10–20	32.0	245	0.62	6.00	3.27	0.24	16	0.74	9.71	5.49	7.10	3.21	24.16	2.42	−26.54	0.70
NFL 2	20–30	31.0	211	3.10	5.48	2.87	0.20	16	0.78	8.73	5.55	7.78	3.40	22.26	2.23	−26.16	0.59
Weighted site mean		**33.1**	**245.0**	**2.4**	**5.6**	**4.4**	**0.3**	**17.0**	**0.7**	**12.5**	**5.6**	**6.8**	**3.9**	**25.5**	**2.0**	**−26.5**	**0.6**
Weighted SD		**3.4**	**34.9**	**1.6**	**0.7**	**2.4**	**0.1**	**1.3**	**0.2**	**6.5**	**0.2**	**1.6**	**1.2**	**4.1**	**0.5**	**0.3**	**0.1**
NFL 3	0–5	24.7	232	3.30	8.19	12.31	0.86	16	0.38	22.53	5.34	5.47	3.25	46.65	2.33	−27.42	0.92
NFL 3	5–10	13.3	209	2.54	6.71	9.76	0.76	15	0.41	27.02	5.57	6.54	2.22	39.72	1.99	−27.10	1.23
NFL 3	10–20	15.3	194	3.65	4.81	12.80	1.05	14	0.37	30.12	5.59	4.55	1.45	46.89	4.69	−27.60	1.80
NFL 3	20–30	17.0	212	2.08	3.66	9.47	0.78	14	0.50	22.05	5.86	4.86	0.84	47.71	4.77	−28.17	1.36
Weighted site mean		**17.1**	**208.7**	**2.9**	**5.3**	**11.1**	**0.9**	**14.7**	**0.4**	**25.6**	**5.6**	**5.1**	**1.7**	**45.9**	**3.9**	**−27.7**	**1.4**
Weighted SD		**4.2**	**14.6**	**0.8**	**1.9**	**1.8**	**0.1**	**1.0**	**0.1**	**4.1**	**0.2**	**0.8**	**1.0**	**3.2**	**1.4**	**0.4**	**0.4**
NFL 4	0–5	26.0	197	2.83	6.25	6.29	0.39	19	0.59	13.15	5.97	6.51	4.21	37.12	1.86	−25.81	−0.80
NFL 4	5–10	22.3	180	1.75	5.05	4.09	0.30	16	0.72	8.71	6.34	7.37	4.55	29.28	1.46	−25.65	0.26
NFL 4	10–20	20.8	170	0.53	3.98	4.29	0.34	15	0.69	10.25	6.45	6.84	4.27	29.76	2.98	−25.53	0.76
NFL 4	20–30	20.2	165	0.49	3.12	3.56	0.30	14	0.75	8.44	6.60	9.45	5.52	26.67	2.67	−25.36	1.06
Weighted site mean		**21.7**	**174.3**	**1.1**	**4.3**	**4.3**	**0.3**	**15.3**	**0.7**	**9.9**	**6.4**	**7.7**	**4.7**	**29.9**	**2.4**	**−25.5**	**0.5**

(Continued on following page)

10.3389/fenvs.2025.1570358

TABLE 2 (*Continued*) Soil properties of non-flooded reference soils. Site means and standard deviations (SD) for each variable and site are included in bold (weighted according to thickness of depth interval of each observation).

Site	Depth cm	POX_{02}-C	POX_{33}-C	MBC	K_2SO_4-C	C (%)	N (%)	C/N	DBD	SOM	pH	Allophane	Ferrihydrite	C Density	C Stock	$\delta^{13}C$	$\delta^{15}N$
		g kg_{carbon}^{-1}				%	%	molar ratio	g cm^{-3}	%		%	%	kg m^{-3}	kg m^{-2}	‰	‰
Weighted SD		**2.3**	**13.0**	**1.0**	**1.3**	**1.1**	**0.0**	**1.9**	**0.1**	**1.9**	**0.2**	**1.4**	**0.7**	**4.0**	**0.7**	**0.2**	**0.7**
NFL 5	0–5	36.0	252	5.88	6.52	6.57	0.46	17	0.66	11.41	5.98	8.00	4.88	43.66	2.18	−26.43	0.54
NFL 5	5–10	24.9	183	2.06	5.90	3.24	0.25	15	0.80	8.05	6.12	10.18	5.83	26.06	1.30	−25.63	1.10
NFL 5	10–20	31.2	204	2.78	5.46	2.09	0.16	15	0.85	6.56	6.32	8.74	5.08	17.79	1.78	−25.45	1.05
NFL 5	20–30	37.0	227	2.70	6.11	1.86	0.14	15	0.91	5.34	6.44	8.31	4.61	16.99	1.70	−25.53	0.99
Weighted site mean		**32.9**	**216.3**	**3.1**	**5.9**	**3.0**	**0.2**	**15.2**	**0.8**	**7.2**	**6.3**	**8.7**	**5.0**	**23.2**	**1.7**	**−25.7**	**1.0**
Weighted SD		**5.0**	**25.6**	**1.4**	**0.4**	**1.9**	**0.1**	**0.7**	**0.1**	**2.4**	**0.2**	**0.8**	**0.5**	**11.2**	**0.3**	**0.4**	**0.2**
NFL 6	0–5	22.2	148	0.00	12.92	0.94	0.11	10	1.03	3.56	5.94	8.52	6.73	9.67	0.48	−22.56	1.60
NFL 6	5–10	31.7	178	0.00	13.29	0.56	0.06	11	1.08	2.70	6.27	6.55	5.48	6.09	0.30	−22.92	1.32
NFL 6	10–20	9.2	133	0.00	10.74	0.54	0.06	11	1.11	2.94	6.48	5.25	4.67	5.92	0.59	−22.36	1.94
NFL 6	20–30	25.6	174	5.33	14.01	0.57	0.06	11	1.10	3.41	6.57	7.45	5.99	6.30	0.63	−22.46	1.86
Weighted site mean		**20.6**	**156.7**	**1.8**	**12.6**	**0.6**	**0.1**	**10.7**	**1.1**	**3.2**	**6.4**	**6.7**	**5.6**	**6.7**	**0.5**	**−22.5**	**1.8**
Weighted SD		**9.8**	**22.6**	**2.9**	**1.6**	**0.2**	**0.0**	**0.2**	**0.0**	**0.4**	**0.3**	**1.4**	**0.9**	**1.5**	**0.1**	**0.2**	**0.3**

10.3389/fenvs.2025.1570358

10.3389/fenvs.2025.1570358

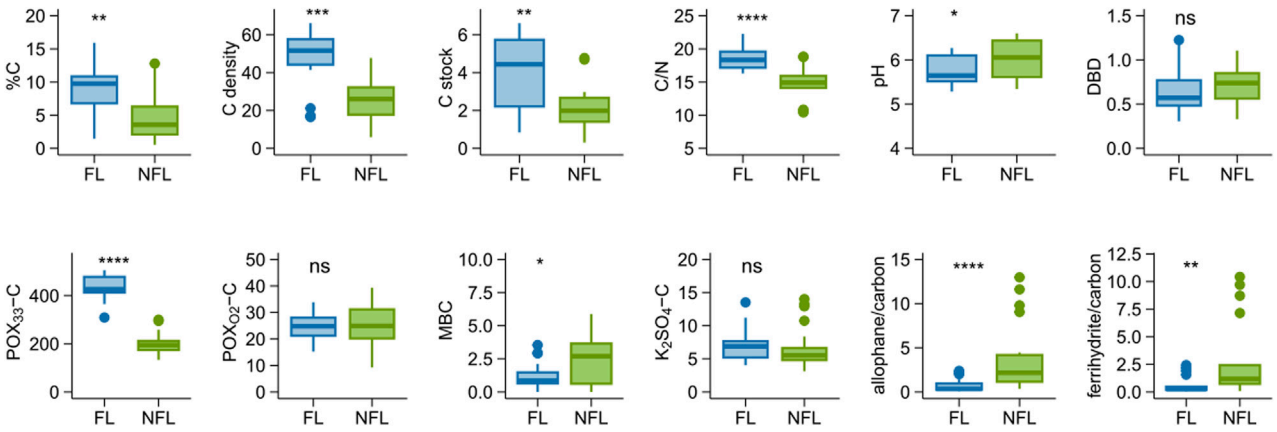

FIGURE 4
Boxplots comparing distribution and means of selected variables of flooded soils (FL) and not flooded reference soils (NFL). Statistical significance is indicated by the following symbols: ns: $p > 0.05$, *: $p \leq 0.05$, **: $p \leq 0.01$, ***: $p \leq 0.001$, ****: $p \leq 0.0001$. Observations are weighted according to thickness of depth interval.

ferrihydrite/carbon was on average 2.47 in the reference soils, but only 0.61 in the drowned soils. Allophane/carbon averaged 3.49 in the reference soils and 0.72 in the flooded soils. pH was 5.77 in average in the flooded soils, compared to 6.06 in the reference soils. There was no significant difference between POX_{02}-C, K_2SO_4-C and DBD between the flooded soils and the reference soils.

At most reference sites, %C and C density decreased with depth, while in the flooded soils, these values were either stable or slightly increased with depth (Table 2; Table 3). Overall, $\delta^{13}C$ and $\delta^{15}N$ values showed little variation with depth. In the reference soils, $\delta^{13}C$ ranged from approximately −22.5‰ to −28‰, and $\delta^{15}N$ values ranged from approximately 2‰ to −0.8‰. In the flooded soils, $\delta^{13}C$ ranged from approximately −26‰ to −29‰, and $\delta^{15}N$ values ranged from approximately 2.8‰ to −0.2‰.

Variable loadings in the PCA (Table 4) showed that pH, allophane, ferrihydrite, C/N ratios and POX_{33}-C contributed most strongly to PC1, while MBC and POX_{33}-C were the main contributors to PC2. The PCA biplot (Figure 5) illustrates a rather clear division between flooded and reference soil samples. Again, variables associated with organic soil phases, particularly POX_{33}-C were more important in the flooded soils, whereas mineral phases such as allophane and ferrihydrite were more dominant in the reference soils.

Beta regression model coefficients (Table 5) for the model $(POX_{33}\text{-}C)_I = ß_1[\log(\text{allophane})] + ß_2[\log(\text{ferrihydrite})] + ß_3(C/N) + ß_4(pH) + \varepsilon_i$ indicate a significant negative effect of log(allophane) and significant positive effects of log(ferrihydrite) and C/N ratios on POX_{33}-C. The effect of the pH on POX_{33}-C was not significant. The pseudo r^2 was 0.72, suggesting that about 70% of variance in POX_{33}-C was explained by the linear combination of these four predictors.

5 Discussion

5.1 C stocks and C densities in flooded compared to reference soils

The flooding for 24 years has altered the C budget of the soils. C stocks, C density and %C were significantly higher in the drowned soils than in the reference soils (Figure 4; Tables 2, 3). These increases in our soils are consistent with previous research following considerably shorter periods of episodic flooding (5 years; Oelbermann and Schiff, 2010), but contradict results of studies on soils submerged for about 8 decades (Félix-Faure et al., 2019a; Félix-Faure et al., 2019b). The %C distribution with depth was rather uniform in our reservoir soils in contrast to the declining trends in the reference soils (Tables 2, 3). Significantly higher C/N ratios in the flooded soils compared to the reference soils suggest vertical movement of organic material from upper, more organic-rich horizons to deeper layers, as well as incorporation of organic material from decaying vegetation submerged during reservoir formation (Oelbermann and Schiff, 2010; Félix-Faure et al., 2019b). Vertical redistribution of colloidal and dissolved organic carbon is also a known process in soils of natural floodplains (Suchara et al., 2021). Additionally, the O horizons of wetland soils and the upper organic-rich horizons in Brown Andosols likely provided some protection against erosion of the submerged soils.

Contrary to Oelbermann and Schiff (2010), we did not observe enrichment of $\delta^{13}C$ and $\delta^{15}N$ with depth in the flooded soils, nor an overall enrichment of $\delta^{13}C$ and $\delta^{15}N$ in flooded soils compared to the reference soils. These either uniform or declining patterns of $\delta^{13}C$ and $\delta^{15}N$ with depth may indicate restricted biological activity and reduced decomposition rates following flooding (Alewell et al., 2011; Krüger et al., 2014), potentially facilitating high C stocks. Alternatively, preferential conservation of certain organic compounds under anaerobic conditions could explain the observed patterns. For instance, decomposition of ^{13}C- and ^{15}N-depleted recalcitrant compounds such as lignin (Benner et al., 1987; Feyissa et al., 2020) by white rot fungi is suppressed in the absence of oxygen (Félix-Faure et al., 2019b). Importantly, interpretation of $\delta^{13}C$ and $\delta^{15}N$ patterns in soils affected by frequent additions of aeolian material of volcanic origin, such as in Iceland, is challenging (Möckel et al., 2024) and still not fully understood. Nutrients and elements that serve as alternative electron acceptors, such as sulphate and Fe are derived from the weathering of tephra, reworked volcanic material and deposited as aerosols during volcanic eruptions (Klaes et al., 2023; Broder et al., 2012; Rose et al., 2004). They exert a strong influence on element cycling and decomposition trajectories, likely affecting isotopic fractionation processes under both aerobic and anaerobic conditions

TABLE 3 Soil properties of flooded soils within the reservoir. Site means and standard deviations (SD) for each variable and site are included in bold (weighted according to thickness of depth interval of each observation).

Site	Depth	POX_{02}-C	POX_{33}-C	MBC	K_2SO_4-C	C (%)	N (%)	C/N	DBD	SOM	pH	Allophane	Ferrihydrite	C Density	C Stock	$\delta^{13}C$	$\delta^{15}N$
	cm	g kg_{carbon}^{-1}				%	%	molar ratio	g cm^{-3}	%		%	%	kg m^{-3}	kg m^{-2}	‰	‰
FL 1	0–5	25.0	432	0.80	5.58	14.44	0.92	18	0.31	30.63	5.31	1.59	1.22	44.22	2.21	−26.48	1.57
FL 1	5–10	29.2	365	0.63	5.15	15.92	1.01	18	0.36	34.05	5.46	1.22	0.91	57.62	2.88	−26.63	1.08
FL 1	10–20	20.3	478	1.47	5.20	9.76	0.59	20	0.57	20.09	5.55	2.99	1.93	55.75	5.57	−28.05	0.47
FL 1	20–30	33.1	431	0.84	5.20	12.95	0.71	22	0.44	27.05	5.43	2.28	1.54	57.33	5.73	−29.09	−0.18
Weighted site mean		**26.8**	**435.7**	**1.0**	**5.3**	**12.6**	**0.8**	**19.8**	**0.4**	**26.5**	**5.5**	**2.2**	**1.5**	**54.7**	**4.6**	**−27.9**	**0.5**
Weighted SD		**6.2**	**43.7**	**0.4**	**0.2**	**2.6**	**0.2**	**1.5**	**0.1**	**5.9**	**0.1**	**0.8**	**0.4**	**5.5**	**1.7**	**1.2**	**0.7**
FL 2	0–5	25.1	482	3.54	7.32	10.96	0.74	17	0.52	20.98	5.29	2.93	2.76	56.47	2.82	−26.87	1.70
FL 2	5–10	24.8	476	0.00	9.54	10.75	0.73	17	0.48	24.00	5.51	2.75	2.33	51.88	2.59	−27.13	1.75
FL 2	10–20	24.1	505	1.15	6.56	10.65	0.73	18	0.48	24.67	5.62	3.94	2.98	51.61	5.16	−27.52	1.50
FL 2	20–30	32.5	483	1.54	6.88	10.85	0.66	19	0.46	24.42	5.61	2.82	2.16	50.19	5.02	−27.97	1.32
Weighted site mean		**27.2**	**488.9**	**1.5**	**7.3**	**10.8**	**0.7**	**18.1**	**0.5**	**23.9**	**5.5**	**3.2**	**2.6**	**52.0**	**4.3**	**−27.5**	**1.5**
Weighted SD		**4.4**	**13.6**	**1.2**	**1.2**	**0.1**	**0.0**	**1.0**	**0.0**	**1.5**	**0.1**	**0.6**	**0.4**	**2.4**	**1.3**	**0.5**	**0.2**
FL 3	0–5	33.8	496	2.95	11.20	1.74	0.10	22	0.96	4.28	5.94	2.49	2.72	16.71	0.84	−26.54	0.16
FL 3	5–10	29.8	495	1.45	9.09	1.46	0.09	20	1.18	3.85	6.02	2.95	3.18	17.25	0.86	−26.89	−0.12
FL 3	10–20	27.7	425	0.61	7.00	1.57	0.10	20	1.05	4.71	6.10	3.75	3.82	16.57	1.66	−26.28	0.54
FL 3	20–30	25.8	413	0.64	6.12	1.73	0.11	20	1.23	3.99	6.15	3.70	3.31	21.16	2.12	−25.88	1.11
Weighted site mean		**28.4**	**444.4**	**1.2**	**7.8**	**1.6**	**0.1**	**20.2**	**1.1**	**4.3**	**6.1**	**3.4**	**3.4**	**18.2**	**1.5**	**−26.3**	**0.6**
Weighted SD		**3.2**	**42.1**	**1.0**	**2.1**	**0.1**	**0.0**	**1.1**	**0.1**	**0.4**	**0.1**	**0.6**	**0.4**	**2.4**	**0.6**	**0.4**	**0.5**
FL 4	0–5	15.2	413	0.85	9.17	8.26	0.60	16	0.58	16.08	5.94	5.00	3.81	47.56	2.38	−26.12	2.77
FL 4	5–10	21.2	426	2.91	13.52	6.79	0.48	17	0.61	15.31	6.19	3.68	2.95	41.44	2.07	−26.39	2.69
FL 4	10–20	19.4	409	0.92	8.88	6.80	0.47	17	0.65	16.20	6.27	6.43	3.26	44.41	4.44	−27.03	1.50
FL 4	20–30	18.9	309	0.68	7.65	7.91	0.53	17	0.77	11.86	6.18	5.56	1.98	60.97	6.10	−27.52	1.29

(Continued on following page)

10.3389/fenvs.2025.1570358

10.3389/fenvs.2025.1570358

TABLE 3 (*Continued*) Soil properties of flooded soils within the reservoir. Site means and standard deviations (SD) for each variable and site are included in bold (weighted according to thickness of depth interval of each observation).

Site	Depth	POX_{02}-C	POX_{33}-C	MBC	K_2SO_4-C	C (%)	N (%)	C/N	DBD	SOM	pH	Allophane	Ferrihydrite	C Density	C Stock	$\delta^{13}C$	$\delta^{15}N$
	cm	g kg_{carbon}^{-1}				%	%	molar ratio	g cm^{-3}	%		%	%	kg m^{-3}	kg m^{-2}	‰	‰
Weighted site mean		**18.9**	**379.1**	**1.2**	**9.3**	**7.4**	**0.5**	**16.8**	**0.7**	**14.6**	**6.2**	**5.4**	**2.9**	**50.0**	**4.3**	**−26.9**	**1.8**
Weighted SD		**2.1**	**57.7**	**0.9**	**2.3**	**0.7**	**0.1**	**0.4**	**0.1**	**2.3**	**0.1**	**1.1**	**0.8**	**9.2**	**1.8**	**0.6**	**0.7**
FL 6	0–5	24.1	426	2.11	7.24	10.21	0.71	17	0.52	21.46	5.66	3.54	3.30	52.91	2.65	−26.32	2.11
FL 6	5–10	24.3	392	0.66	7.00	9.56	0.66	17	0.63	19.05	5.65	3.57	2.44	59.97	3.00	−26.25	1.79
FL 6	10–20	23.8	425	0.51	4.75	10.67	0.71	18	0.62	18.60	5.71	3.07	2.11	66.04	6.60	−26.98	0.69
FL 6	20–30	28.0	458	1.20	4.02	11.99	0.75	19	0.48	27.95	5.52	2.84	1.59	58.03	5.80	−27.32	0.22
Weighted site mean		**25.3**	**430.6**	**1.0**	**5.3**	**10.8**	**0.7**	**17.7**	**0.6**	**22.3**	**5.6**	**3.2**	**2.2**	**60.2**	**5.1**	**−26.9**	**1.0**
Weighted SD		**2.2**	**26.0**	**0.7**	**1.5**	**1.0**	**0.0**	**0.9**	**0.1**	**4.8**	**0.1**	**0.3**	**0.7**	**5.4**	**1.9**	**0.5**	**0.9**

(Möckel et al., 2024). Further research is needed to better understand the influence of volcanic ejecta on element cycling and on the depth patterns of $\delta^{13}C$ and $\delta^{15}N$ values in volcanic soils.

5.2 Properties of organic and mineral soil constituents in flooded compared to reference soils

Content of POX_{33}-C was considerably higher in the flooded soils than in the reference soils (Figure 4; Tables 2 and 3), which may be partly explained by a lower content of mineral phases in the flooded compared to the reference soils. This could render the C of the flooded soils less protected by mineral soil colloids and, hence, more sensitive to oxidation. Our findings of a negative influence of allophane/carbon content on POX_{33}-C (p = 0.0003; Table 5) are consistent with Tirol-Padre and Ladha (2004), who observed no significant correlation between clay/carbon alone and POX_{33}-C alone, but a negative correlation between silt/carbon and (silt + clay)/carbon and POX_{33}-C. While allophane is a clay-sized mineral, it forms silt-sized aggregates, facilitating C stabilization in two ways: through organo-mineral associations and by the entrapment of SOM within microcompartments that form alongside the silt-sized soil aggregates.

The positive relationship between the ferrihydrite/carbon and POX_{33}-C (p = 0.003; Table 5) is surprising. We would have expected a negative relationship between this clay-sized mineral and the C oxidizable by 33 mM $KMnO_4$. One possible explanation may be the nature of the C stabilized by clay-sized minerals, as pedogenic minerals are known to form preferential bonds with certain C groups. Also, previous studies (e.g., Skjemstad et al., 2006, and references therein) have demonstrated that certain C compounds, namely, aromatic and phenolic structures, are particularly sensitive to oxidation by $KMnO_4$. Interestingly, research in Icelandic Histosol with andic and vitric soil properties indicates a preferential stabilization of phenolic and aromatic C by allophane (Möckel et al., 2021; Möckel et al., 2023). Filimonova et al. (2016) also found enrichment of aromatic C in ferrihydrite associated C, but research in Iceland suggests a preferential stabilization of labile C groups such as O/N-alkyl C by ferrihydrite (Möckel et al., 2021; Möckel et al., 2023). Perhaps allophane has a stronger stabilizing effect on C groups that are more prone to oxidation by $KMnO_4$ than ferrihydrite in our soils. Consequently, only the loss of allophane from the flooded soils may contribute to the higher POX_{33}-C values. Ferrihydrite may generally not play as strong a role for C stabilization as allophane in our soils, similar to previous studies (e.g., Basile-Doelsch et al., 2007), which report approximately a 3.5-fold higher capacity for SOM stabilization by imogolite-type minerals than by Fe oxides. Nonetheless, it remains surprising that ferrihydrite/carbon and POX_{33}-C show a positive relationship in the beta regression (p = 0.003; Table 5) rather than a weak negative or a non-significant association. Without further in-depth studies, we can only hypothesize about the causes. Our results may simply reflect an artefact of the relatively small sample size. Additionally, the effect of changes in clay-sized soil mineral phases may be blurred or overridden by differences in C composition between flooded and reference soils due to inputs of C to the reservoir soils from drowned vegetation.

10.3389/fenvs.2025.1570358

TABLE 4 Loadings show contributions of the different variables to PC1 and PC2. Values of pH, allophane, ferrihydrite, C/N ratios and POX_{33}-C contribute strongly to PC1, MBC and POX_{33}-C contribute strongest to PC2.

	PC1	PC2
POX_{33}-C	−0.376	−0.271
MBC	−0.162	0.881
K_2SO_4-C	−0.159	−0.248
allophane	0.458	−0.081
ferrihydrite	0.440	−0.113
C/N	−0.342	0.087
DBD	0.146	−0.021
pH	0.474	0.184

TABLE 5 Beta regression model coefficients (mean model with logit link) for the model $(POX_{33}\text{-}C)_i = ß_1[\log(\text{allophane/carbon})] + ß_2[\log(\text{ferrihydrite/carbon})] + ß_3(C/N) + ß_4(pH) + \varepsilon_i$. In the model, POX_{33}-C was used as a proportion of total carbon, allophane and ferrihydrite were used as a ratio to total carbon. Pseudo r^2 = 0.72.

	Estimate	Std. Error	z value	Pr(>|z|)
Intercept	−2.1317	1.2834	−1.6610	0.0967
log(allophane/carbon)	−0.6614	0.1813	−3.6490	0.0003
log(ferrihydrite/carbon)	0.4767	0.1579	3.0190	0.0025
C/N	0.1003	0.0249	4.0240	0.0001
pH	−0.0278	0.2003	−0.1390	0.8896

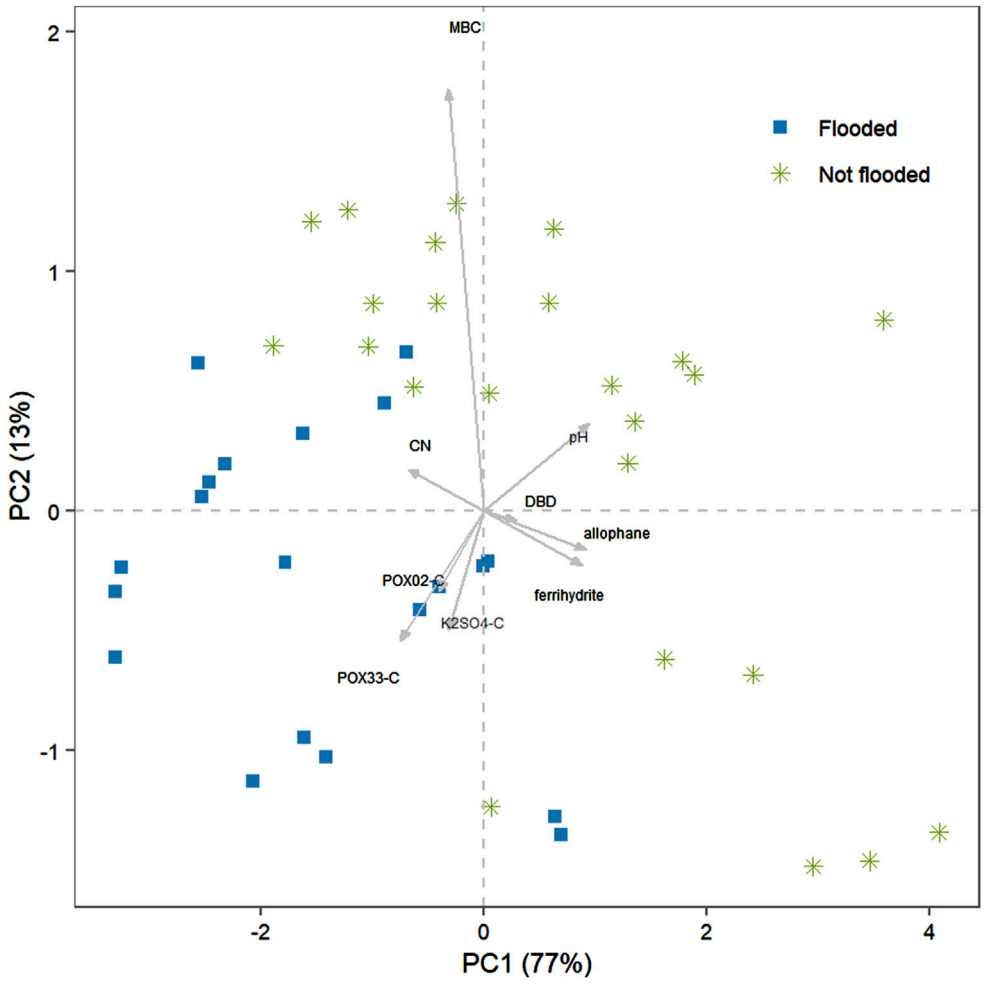

FIGURE 5
Biplot of robust PCA showing variation in organo-mineral composition of the soils, including three external variables (Box-Cox transformed C/N ratios, log transformed DBD, and pH). Variable loadings were multiplied by 2 for better visualization.

As discussed above, C derived from drowned terrestrial vegetation likely led to an increase in C/N ratios of the soils (Félix-Faure et al., 2019b), and simultaneously increased the pool of POX_{33}-C. This is supported by the positive relationship between C/N ratios and POX_{33}-C (p = 0.0001; Table 5), and supports the argument by Tirol-Padre and Ladha (2004) that changes in management practices may alter the pool of C oxidizable by 33 mM $KMnO_4$.

The pH of the soils, which was significantly lower in the reservoir than in the reference soils (Figure 4; Tables 2, 3) showed no significant effect on POX_{33}-C (Table 5, $p = 0.8896$). Though indirect, the influence of pH on C stocks is nonetheless important. The pH of a soil reflects its general chemical condition and controls many soil properties and processes, that influence SOM dynamics (Rasmussen et al., 2018) – including the surface charge and reactivity of minerals, the formation of organo-mineral complexes, and microbial activity. For example, formation of allophane is inhibited at pH < 5, and Neculman et al. (2013) reported that allophane complexation occurs predominantly at pH > 6. Therefore, the significantly lower pH in the flooded soils likely reduces the capacity of allophane to form stable bonds with SOM. Lower pH in the drowned soil could also affect SOM decomposition by influencing decomposer communities, such as microbial composition and activity. Overall, microbial decomposer activity is favoured by a pH range of approximately 5–7 (Wang and Kuzyakov, 2024).

5.3 Long-term implications of changes in soil properties for the carbon balance of submerged soils

Recently, a nexus approach to address challenges such as secure access to resources like water, food and energy, or to ensure peace has gained attention. The nexus approach emphasizes the interrelations between different natural resources and their connection to socioeconomic challenges (Lal et al., 2017; Lal, 2015). As explained by Hatfield et al. (2017) and Lal et al. (2017) soils are often a neglected link of this approach. They argue that soils should be at the center of the interrelation between water, food and energy. While they explain well why soil health and soil functioning is key to energy security, potential ramifications of energy production for soil resources are not discussed.

Our study adds to the emerging body of research addressing the consequences of hydroelectric infrastructure such as reservoir flooding on soils. The inundation of the Blöndulón reservoir area caused profound changes in the physicochemical properties of the drowned soils. Relative C contents, C stocks and C density were significantly higher compared to the reference soils (Figure 4; Tables 2, 3), likely due to C inputs from the drowned terrestrial vegetation. Conceivably, this imposes a high risk of elevated C losses in the coming decades as the increased C levels appear to be less protected by mineral phases and more sensitive to oxidation than C in the reference soils. Under continued inundation by the hydropower reservoir, C loss may occur both in form of CO_2 and CH_4 due to mineralization (Huttunen et al., 2002; Wang et al., 2024), as well as through erosion. High energy waves and waves during low water levels can erode sediments and submerged soils in the nearshore environment (Vilmundardóttir et al., 2010), and in the annual drawdown zone (Félix-Faure et al., 2019a; Félix-Faure et al., 2019b). When strong dry winds that are-common in Iceland (Figure 2A) coincide with exposure of the reservoir soils, wind erosion becomes likely (Vilmundardóttir et al., 2010). Similarly, long-term exposure of the submerged soils, e.g., following dam removal, could render the C of the drowned soils vulnerable to losses via mineralization and, in the absence of a protective vegetation cover, to losses by erosion (Foley et al., 2017). Therefore, future dam removal, which may be driven by concerns about safety or economic reasons when dams age, or by a call for environmental reconstruction (Vahedifard et al., 2021), must consider the vulnerability of the exposed soils. Dam removal should go hand in hand with interventive measures to prevent detrimental side effects, such as soil loss from the impoundment area and sandification of surrounding land. Finally, more research is needed on the environmental impacts of reservoir impoundments in Iceland - a country which increasingly relies on hydropower. Future studies should focus on GHG emissions from hydroelectric reservoirs and the long-term fate of the C stored in flooded lands.

Data availability statement

The original contributions presented in the study are included in the article/supplementary material, further inquiries can be directed to the corresponding author.

Author contributions

SM: Conceptualization, Formal Analysis, Investigation, Methodology, Supervision, Visualization, Writing – original draft, Writing – review and editing. TB: Conceptualization, Investigation, Methodology, Supervision, Writing – review and editing. EE: Conceptualization, Methodology, Project administration, Supervision, Writing – review and editing. IÁ: Investigation, Methodology, Writing – review and editing. UM: Investigation, Methodology, Writing – review and editing. GG: Conceptualization, Funding acquisition, Project administration, Resources, Supervision, Writing – original draft.

Funding

The author(s) declare that financial support was received for the research and/or publication of this article. This research was funded by Landsvirkjun, the national power company of Iceland.

Acknowledgments

We would like to thank Þorsteinn Jónsson, Höskuldur Þorbjarnarson, and Sigrún Dögg Eddudóttir for assistance with field work. The Blönduvirkjun hydropower plant kindly hosted us during fieldwork.

Conflict of interest

The authors declare that the research was conducted in the absence of any commercial or financial relationships that could be construed as a potential conflict of interest.

Generative AI statement

The author(s) declare that no Generative AI was used in the creation of this manuscript.

Publisher's note

References

Agricultural Research Institute (1970). "Gróðurkort af Íslandi," in *Blað 187 friðmundarvötn; blað 188 suaðafell*, 1. 40 000. Reykjavík: Menningarsjóður.

Alessi, D. S., Walsh, D. M., and Fein, J. B. (2011). Uncertainties in determining microbial biomass C using the chloroform fumigation–extraction method. *Chem. Geol.* 280, 58–64. doi:10.1016/j.chemgeo.2010.10.014

Alewell, C., Giesler, R., Klaminder, J., Leifeld, J., and Rollog, M. (2011). Stable carbon isotopes as indicators for environmental change in palsa peats. *Biogeosciences* 8, 1769–1778. doi:10.5194/bg-8-1769-2011

Arnalds, Ó. (2015). *The soils of Iceland*. Springer Netherlands.

Arnalds, Ó., and Óskarsson, H. (2009). Íslenskt jarðvegskort. *Náttúrufræðingurinn* 78, 107–121.

Arnalds, O., Thorarinsdottir, E., Metúsalemsson, S., Jonsson, A., Gretarsson, E., and Arnason, A. (2001). Soil erosion in Iceland, reykjavik, soil conservation service and agricultural research Institute.

Asano, M., and Wagai, R. (2014). Evidence of aggregate hierarchy at micro-to submicron scales in an allophanic Andisol. *Geoderma* 216, 62–74. doi:10.1016/j.geoderma.2013.10.005

Banach, A. M., Banach, K., Peters, R. C. J. H., Jansen, R. H. M., Visser, E. J. W., Stępniewska, Z., et al. (2009). Effects of long-term flooding on biogeochemistry and vegetation development in floodplains; a mesocosm experiment to study interacting effects of land use and water quality. *Biogeosciences* 6, 1325–1339. doi:10.5194/bg-6-1325-2009

Basile-Doelsch, I., Amundson, R., Stone, W. E. E., Borschneck, D., Bottero, J. Y., Moustier, S., et al. (2007). Mineral control of carbon pools in a volcanic soil horizon. *Geoderma* 137, 477–489. doi:10.1016/j.geoderma.2006.10.006

Benner, R., Fogel, M. L., Sprague, E. K., and Hodson, R. E. (1987). Depletion of 13C in lignin and its implications for stable carbon isotope studies. *Nature* 329, 708–710. doi:10.1038/329708a0

Blakemore, L. C., Searle, P. L., and Daly, B. K. (1987). *Methods for chemical analysis of soils, NZ soil bureau*. Department of Scientific and Industrial Research.

Bonatotzky, T., Ottner, F., Erlendsson, E., and Gísladóttir, G. (2021). Weathering of tephra and the formation of pedogenic minerals in young Andosols, South East Iceland. *CATENA* 198, 105030–105115. doi:10.1016/j.catena.2020.105030

Broder, T., Blodau, C., Biester, H., and Knorr, K. H. (2012). Peat decomposition records in three pristine ombrotrophic bogs in southern Patagonia. *Biogeosciences* 9, 1479–1491. doi:10.5194/bg-9-1479-2012

Buytaert, W., Célleri, R., De Bièvre, B., Cisneros, F., Wyseure, G., Deckers, J., et al. (2006). Human impact on the hydrology of the Andean páramos. *Earth-Science Rev.* 79, 53–72. doi:10.1016/j.earscirev.2006.06.002

Candan, F., and Broquen, P. (2009). Aggregate stability and related properties in NW Patagonian Andisols. *Geoderma* 154, 42–47. doi:10.1016/j.geoderma.2009.09.010

Chanudet, V., Guédant, P., Rode, W., Godon, A., Guérin, F., Serça, D., et al. (2016). Evolution of the physico-chemical water quality in the Nam Theun 2 Reservoir and downstream rivers for the first 5 years after impoundment. *Hydroécologie Appliquée* 19, 27–61. doi:10.1051/hydro/2015001

Chen, C., Hall, S. J., Coward, E., and Thompson, A. (2020). Iron-mediated organic matter decomposition in humid soils can counteract protection. *Nat. Commun.* 11, 2255–2313. doi:10.1038/s41467-020-16071-5

Childs, C. W. (1985). *Towards understanding soil mineralogy II. Notes on ferrihydrite. N.Z. Soil Bureau Laboratory Report CM7*. Lower Hutt, New Zealand: NZ Soil Bureau.

Cribari-Neto, F., and Zeileis, A. (2010). Beta regression in R. *J. Stat. Softw.* 34, 1–24. doi:10.18637/jss.v034.i02

De Souza, J. A. M. (1996). "Brazil and the UN framework convention on climate change. In: International atomic energy agency (ed.) Comparison of Energy Sources in Terms of their Full-Chain Emission Factors," in Proceedings of an IAEA Advisory Group Meeting/Workshop held in Beijing, China, October 4–7, 1994 (Vienna, Austria: International Atomic Energy Agency).

European Environment Agency (2019). EUNIS database. Available online at: https://eunis.eea.europa.eu/index.jsp (Accessed April 27, 2025).

Félix-Faure, J., Gaillard, J., Descloux, S., Chanudet, V., Poirel, A., Baudoin, J.-M., et al. (2019a). Contribution of flooded soils to sediment and nutrient fluxes in a hydropower reservoir (sarrans, Central France). *Ecosystems* 22, 312–330. doi:10.1007/s10021-018-0274-9

Félix-Faure, J., Walter, C., Balesdent, J., Chanudet, V., Avrillier, J.-N., Hossann, C., et al. (2019b). Soils drowned in water impoundments: a new frontier. *Front. Environ. Sci.* 7, 1–15. doi:10.3389/fenvs.2019.00053

Feyissa, A., Yang, F., Feng, J., Wu, J., Chen, Q., and Cheng, X. (2020). Soil labile and recalcitrant carbon and nitrogen dynamics in relation to functional vegetation groups along precipitation gradients in secondary grasslands of South China. *Environ. Sci. Pollut. Res.* 27, 10528–10540. doi:10.1007/s11356-019-07583-9

Filimonova, S., Kaufhold, S., Wagner, F. E., Häusler, W., and Kögel-Knabner, I. (2016). The role of allophane nano-structure and Fe oxide speciation for hosting soil organic matter in an allophanic Andosol. *Geochim. Cosmochim. Acta* 180, 284–302. doi:10.1016/j.gca.2016.02.033

Filzmoser, P., Hron, K., and Templ, M. (2018). *Applied compositional data analysis. With worked examples in R*. Springer.

Foley, M. M., Bellmore, J. R., O'connor, J. E., Duda, J. J., East, A. E., Grant, G. E., et al. (2017). Dam removal: listening in. *Water Resour. Res.* 53, 5229–5246. doi:10.1002/2017WR020457

Guicharnaud, R., Arnalds, O., and Paton, G. I. (2010). Short term changes of microbial processes in Icelandic soils to increasing temperatures. *Biogeosciences* 7, 671–682. doi:10.5194/bg-7-671-2010

Hatfield, J. L., Sauer, T. J., and Cruse, R. M. (2017). "Chapter one - soil: the forgotten piece of the water, food, energy nexus," in *Advances in agronomy*. Editor D. L. SPARKS (Academic Press).

Heiri, O., Lotter, A. F., and Lemcke, G. (2001). Loss on ignition as a method for estimating organic and carbonate content in sediments: reproducibility and comparability of results. *J. Paleolimnol.* 25, 101–110. doi:10.1023/a:1008119611481

Hewitt, A. E., Lowe, D. J., and Balks, M. R. (2021). *The soils of aotearoa New Zealand*. Springer International Publishing.

Huttunen, J., Tero, S., Hellsten, S., Heikkinen, M., Nykänen, H., Jungner, H., et al. (2002). Fluxes of CH4, CO2, and N2O in hydroelectric reservoirs Lokka and Porttipahta in the northern boreal zone in Finland. *Glob. Biogeochem. Cycles* 16, 1–17. doi:10.1029/2000GB001316

Inagaki, T. M., Possinger, A. R., Grant, K. E., Schweizer, S. A., Mueller, C. W., Derry, L. A., et al. (2020). Subsoil organo-mineral associations under contrasting climate conditions. *Geochim. Cosmochim. Acta* 270, 244–263. doi:10.1016/j.gca.2019.11.030

Iuss Working Group Wrb (2022). *World Reference Base for Soil Resources. International soil classification system for naming soils and creating legends for soil maps*. 4th edition. Vienna, Austria: International Union of Soil Sciences IUSS.

Iversen, C. M., Sloan, V. L., Sullivan, P. F., Euskirchen, E. S., Mcguire, A. D., Norby, R. J., et al. (2015). The unseen iceberg: plant roots in arctic tundra. *New Phytol.* 205, 34–58. doi:10.1111/nph.13003

Kaldal, I., and Víkingsson, S. (1982). "Blönduvirkjun: jarðgrunnur á lónstæði og mat á áhrifum lónsins á jarðvegseyðingu, Reykjavík,". Orkustofnun.

Klaes, B., Thiele-Bruhn, S., Wörner, G., Höschen, C., Mueller, C. W., Marx, P., et al. (2023). Iron (hydr)oxide formation in Andosols under extreme climate conditions. *Sci. Rep.* 13, 2818–2917. doi:10.1038/s41598-023-29727-1

Kleber, M., Mikutta, R., Torn, M. S., and Jahn, R. (2005). Poorly crystalline mineral phases protect organic matter in acid subsoil horizons. *Eur. J. Soil Sci.* 56, 717–725. doi:10.1111/j.1365-2389.2005.00706.x

Knorr, K. H. (2013). DOC-dynamics in a small headwater catchment as driven by redox fluctuations and hydrological flow paths – are DOC exports mediated by iron reduction/oxidation cycles? *Biogeosciences* 10, 891–904. doi:10.5194/bg-10-891-2013

Kögel-Knabner, I., and Amelung, W. (2021). Soil organic matter in major pedogenic soil groups. *Geoderma* 384, 1–22. doi:10.1016/j.geoderma.2020.114785

Kögel-Knabner, I., Guggenberger, G., Kleber, M., Kandeler, E., Kalbitz, K., Scheu, S., et al. (2008). Organo-mineral associations in temperate soils: integrating biology, mineralogy, and organic matter chemistry. *J. Plant Nutr. Soil Sci.* 171, 61–82. doi:10.1002/jpln.200700048

Kristinsson, H. (2010). *Íslenska plöntuhandbókin: blómplöntur og byrkningar, Reykjavík, Mál og Menning.*

Kristinsson, H., and Hallgrímsson, H. (1978). *Náttúruverndarkönnun á virkjunarsvæði Blöndu*. Orkustofnun.

Krüger, J. P., Leifeld, J., and Alewell, C. (2014). Degradation changes stable carbon isotope depth profiles in palsa peatlands. *Biogeosciences* 11, 3369–3380. doi:10.5194/bg-11-3369-2014

Kuhry, P., and Vitt, D. H. (1996). Fossil carbon/nitrogen ratios as a measure of peat decomposition. *Ecology* 77, 271–275. doi:10.2307/2265676

Lal, R. (2015). The soil–peace nexus: our common future. *Soil Sci. Plant Nutr.* 61, 566–578. doi:10.1080/00380768.2015.1065166

Lal, R., Mohtar, R. H., Assi, A. T., Ray, R., Baybil, H., and Jahn, M. (2017). Soil as a basic nexus tool: soils at the center of the food–energy–water nexus. *Curr. Sustainable/Renewable Energy Rep.* 4, 117–129. doi:10.1007/s40518-017-0082-4

Malmer, N., and Holm, E. (1984). Variation in the C/N-quotient of peat in relation to decomposition rate and age determination with 210Pb. *Oikos* 43, 171–182. doi:10.2307/3544766

Martín-Fernández, J. A., Hron, K., Templ, M., Filzmoser, P., and Palarea-Albaladejo, J. (2012). Model-based replacement of rounded zeros in compositional data: classical and robust approaches. *Comput. Stat. & Data Anal.* 56, 2688–2704. doi:10.1016/j.csda.2012.02.012

Mizota, C., and Van Reeuwijk, L. P. (1989). "Clay mineralogy and chemistry of soils formed in volcanic material in diverse climatic regions," in *Soil monograph* (Wageningen: ISRIC), 2.

Möckel, S. C., Erlendsson, E., and Gísladóttir, G. (2021). Andic soil properties and tephra layers hamper C turnover in Icelandic peatlands. *J. Geophys. Res. Biogeosci.* 126, 1–20. doi:10.1029/2021JG006433

Möckel, S. C., Erlendsson, E., and Gísladóttir, G. (2023). Effect of mineral soil constituents on carbon characteristics of peatlands in aeolian environments of Iceland. *Wetl. Ecol. Manag.* 31, 853–874. doi:10.1007/s11273-023-09956-x

Möckel, S. C., Erlendsson, E., and Gísladóttir, G. (2024). Depth trends of δ13C and δ15N values in peatlands in aeolian environments of Iceland. *Wetlands* 44, 42. doi:10.1007/s13157-024-01796-6

Mueller-Dombois, D., and Ellenberg, H. (1974). *Aims and methods of vegetation ecology*. New York: John Wiley & Sons.

Mulligan, M., Van Soesbergen, A., and Sáenz, L. (2020). GOODD, a global dataset of more than 38,000 georeferenced dams. *Sci. Data* 7, 31. doi:10.1038/s41597-020-0362-5

Nanzyo, M., Dahlgren, R., and Shoji, S. (1993). "Chapter 6: chemical characteristics of volcanic ash soils," in *Volcanic ash soils - genesis, properties and utilization. Developments in soil science*. Editors S. Shoji, M. Nanzyo, and R. A. Dahlgren (Amsterdam, London, New York, Tokyo: Elsevier Science).

Neculman, R., Rumpel, C., Matus, F., Godoy, R., Steffens, M., and De La Luz Mora, M. (2013). Organic matter stabilization in two Andisols of contrasting age under temperate rain forest. *Biol. Fertil. Soils* 49, 681–689. doi:10.1007/s00374-012-0758-2

Oelbermann, M., and Schiff, S. L. (2008). Quantifying carbon dioxide and methane emissions and carbon dynamics from flooded boreal forest soil. *J. Environ. Qual.* 37, 2037–2047. doi:10.2134/jeq2008.0027

Oelbermann, M., and Schiff, S. L. (2010). The redistribution of soil organic carbon and nitrogen and greenhouse gas production rates during reservoir drawdown and reflooding. *Soil Sci.* 175, 72–80. doi:10.1097/SS.0b013e3181ce0453

Orkustofnun (2022a). Orkutölur 2021/energy in numbers 2021. Available online at: https://orkustofnun.is/upplysingar/orkutolur (Accessed April 27, 2025).

Orkustofnun (2022b). OS-2022-T003-01: Þróun raforkuframleiðslu á Íslandi (2021)/OS-2022-T003-01: development of electricity production in Iceland. Available online at: https://orkustofnun.is/upplysingar/talnaefni/raforka (Accessed April 27, 2025).

Orkustofnun (2023). OS-2023-T011-01: frumorkunotkun á íslandi 1940-2022/OS-2023-T011-01: primary energy use in Iceland 1940-2022. *Orkustofnun Data Repos. OS-2023-T011-01*. Available online at: https://orkustofnun.is/upplysingar/talnaefni/orka (Accessed April 27, 2025).

Parfitt, R. L., and Wilson, A. D. (1985). Estimation of allophane and halloysite in three sequences of volcanic soils, New Zealand. *Volcan. Soils Catena Suppl.* 7, 1–8.

Rasmussen, C., Heckman, K., Wieder, W. R., Keiluweit, M., Lawrence, C. R., Berhe, A. A., et al. (2018). Beyond clay: towards an improved set of variables for predicting soil organic matter content. *Biogeochemistry* 137, 297–306. doi:10.1007/s10533-018-0424-3

Rayment, G. E., and Lyons, D. J. (2011). *Soil chemical methods - australasia*. Collingwood: Csiro Publishing.

Rose, W. I., Gu, Y., Watson, I. M., Yu, T., Blut, G. J. S., Prata, A. J., et al. (2004). "The February–March 2000 eruption of Hekla, Iceland from a satellite perspective," in *Volcanism and the earth's atmosphere*. Editors A. Robock and C. Oppenheimer (American Geophysical Union).

Scheffran, J., Felkers, M., and Froese, R. (2020). "Economic growth and the global energy demand," in *Green energy to sustainability*. Editors A. A. Vertes, N Qureshi, H. P. Blaschek, and H. Yukawa (John Wiley & Sons).

Schoeneberger, P. J., Wysocki, D. A., Benham, E. C., and Stuff, S. S. (2012). *Field book for describing and sampling soils, version 3.0, lincoln, new England, national soil Survey center, natural resources conservation service*. Washington: U.S. Department of Agriculture.

Shoji, S., Dahlgren, R., and Nanzyo, M. (1993). "Chapter 3: genesis of volcanic ash soils," in *Volcanic ash soils - genesis, properties and utilization. Developments in soil science*. Editors S. Shoji, M. Nanzyo, and R. DAHLGREN (Amsterdam, London, New York, Tokyo: Elsevier Science).

Skjemstad, J. O., Swift, R. S., and Mcgowan, J. A. (2006). Comparison of the particulate organic carbon and permanganate oxidation methods for estimating labile soil organic carbon. *Soil Res.* 44, 255–263. doi:10.1071/SR05124

Soil Survey Staff (2014). "Kellogg soil Survey laboratory methods manual," in *Soil Survey investigations report no. 42, version 5.0, U.S. Department of agriculture, natural resources conservation service*. National Soil Survey Center, Lincoln, Nebraska: Kellogg Soil Survey Laboratory.

Strawn, D. G., Bohn, H. L., and O'connor, G. A. (2015). "Redox reactions in soils," in *Soil chemistry*. Editors D. G. Strawn, H. L. Bohn, and G. A. O'Connor (UK: John Wiley & Sons).

Suchara, I., Sucharova, J., and Hola, M. (2021). Changes in selected physico-chemical properties of floodplain soils in three different land-use types after flooding. *Plant, Soil Environ.* 67, 99–109. doi:10.17221/435/2020-PSE

Takahashi, T., and Dahlgren, R. A. (2016). Nature, properties and function of aluminum–humus complexes in volcanic soils. *Geoderma* 263, 110–121. doi:10.1016/j.geoderma.2015.08.032

Templ, M., Hron, K., and Filzmoser, P. (2011). "robCompositions: an R-package for robust statistical analysis of compositional data," in *Compositional data analysis: theory and applications*. Editors V. Pawlowsky-Glahn and A. Buccianti (John Wiley & Sons, Ltd).

Tirol-Padre, A., and Ladha, J. K. (2004). Assessing the reliability of permanganate-oxidizable carbon as an index of soil labile carbon. *Soil Sci. Soc. Am. J.* 68, 969–978. doi:10.2136/sssaj2004.9690

Unger, I. M., Kennedy, A. C., and Muzika, R.-M. (2009). Flooding effects on soil microbial communities. *Appl. Soil Ecol.* 42, 1–8. doi:10.1016/j.apsoil.2009.01.007

United Nations (2023). *The sustainable development goals report 2023*. Special edition. United Nations.

Vahedifard, F., Madani, K., Aghakouchak, A., and Thota, S. K. (2021). Are we ready for more dam removals in the United States? *Environ. Res. Infrastruct. Sustain.* 1, 013001–013006. doi:10.1088/2634-4505/abe639

Vance, E. D., Brookes, P. C., and Jenkinson, D. S. (1987). An extraction method for measuring soil microbial biomass C. *Soil Biol. Biochem.* 19, 703–707. doi:10.1016/0038-0717(87)90052-6

Van Den Boogaart, K. G., and Tolosana-Delgado, R. (2013). *Analyzing compositional data with R*. Berlin-Heidelberg: Springer.

Vilmundardóttir, O. K., Gísladóttir, G., and Lal, R. (2014). Early stage development of selected soil properties along the proglacial moraines of Skaftafellsjökull glacier, SE-Iceland. *Catena* 121, 142–150. doi:10.1016/j.catena.2014.04.020

Vilmundardóttir, O. K., Magnússon, B., Gísladóttir, G., and Thorsteinsson, T. (2010). Shoreline erosion and aeolian deposition along a recently formed hydro-electric reservoir, Blöndulón, Iceland. *Geomorphology* 114, 542–555. doi:10.1016/j.geomorph.2009.08.012

Voegeli, G., and Finger, D. C. (2021). Disputed dams: mapping the divergent stakeholder perspectives, expectations, and concerns over hydropower development in Iceland and Switzerland. *Energy Res. & Soc. Sci.* 72, 101872–101923. doi:10.1016/j.erss.2020.101872

Wada, K. (1985). "The distinctive properties of Andosols," in *Advances in soil science*. Editor B. A. Stewart (New York, NY: Springer).

Wada, K. (1989). "Allophane and imogolite," in *Minerals in soil environment. SSSA book series 1*. Editors J. B. Dixon and S. B. Weed (Madison, Wisconsin, USA: Soil Science Society of America).

Wang, C., and Kuzyakov, Y. (2024). Soil organic matter priming: the pH effects. *Glob. Change Biol.* 30, 173499–e17421. doi:10.1111/gcb.17349

Wang, Z., Chan, F. K. S., Feng, M., and Johnson, M. F. (2024). Greenhouse gas emissions from hydropower reservoirs: emission processes and management approaches. *Environ. Res. Lett.* 19, 073002. doi:10.1088/1748-9326/ad560c

Weil, R. R., Islam, K. R., Stine, M. A., Gruver, J. B., and Samson-Liebig, S. E. (2003). Estimating active carbon for soil quality assessment: a simplified method for laboratory and field use. *Am. J. Altern. Agric.* 18, 3–17. doi:10.1079/AJAA200228

Wright, H. E. (1967). A square-rod piston sampler for lake sediments. *J. Sediment. Res.* 37, 975–976. doi:10.1306/74D71807-2B21-11D7-8648000102C1865D

Zarfl, C., Lumsdon, A. E., Berlekamp, J., Tydecks, L., and Tockner, K. (2015). A global boom in hydropower dam construction. *Aquat. Sci.* 77, 161–170. doi:10.1016/j.scitotenv.2020.143108

Zhang, H., Tuittila, E.-S., Korrensalo, A., Laine, A. M., Uljas, S., Welti, N., et al. (2021). Methane production and oxidation potentials along a fen-bog gradient from southern boreal to subarctic peatlands in Finland. *Glob. Change Biol.* 27, 4449–4464. doi:10.1111/gcb.15740

Zhu, K., Ran, Y., Ma, M., Li, W., Mir, Y., Ran, J., et al. (2022). Ameliorating soil structure for the reservoir riparian: the influences of land use and dam-triggered flooding on soil aggregates. *Soil Tillage Res.* 216, 105263–105313. doi:10.1016/j.still.2021.105263